Backgrounds Due to the Formation of Super-massive Black Holes in the Early Universe

Peter L. Biermann[1, 2, 3, 4] and Benjamin C. Harms[1]

[1] *Department of Physics and Astronomy, The University of Alabama, Box 870324, Tuscaloosa, AL 35487-0324, USA*

[2] *MPI for Radioastronomy, Bonn, Germany*

[3] *Institut für Kernphysik - Karlsruhe Institute of Technology (KIT) , Germany*

[4] *Department of Physics & Astronomy, University of Bonn, Germany*

MNRAS 441, 1147(2014); MNRAS 466, L34(2017)

Radio Synchrotron Background Workshop

July 2017

plbiermann@mpifr-bonn.mpg.de

bharms@ua.edu

Outline of Talk

Introduction

Our Model of Non-thermal Radio Background

Observational Checks

Additional Features of the Model

Conclusions

Introduction

Isotropic Radio frequency background

An isotropic radio background of unknown origin has been detected by several groups.

If this excess is not an artifact of an over-simplified model of galactic geometry, what is the cause of the excess?

Formation of super-massive black holes at high redshift

Super-massive stars may form at high redshift ($z \sim 50$) when metallicity is low.

Supernovae explosions of massive Population III stars could lead to the first generation of black holes. Massive stars form in dense groups, so stars could agglomerate to form super-massive stars.

Super-massive black holes may have started forming at a redshift of $z \sim 50$.

Non-thermal Radio Background

First generation of super-massive black holes

Black holes produced by exploding super-massive stars

The explosion of a super-massive star is modeled as an ordinary supernova explosion scaled-up to the energy of the super-massive star.

In the Sedov-Taylor phase the radius of a blast wave originating at a redshift z_0 is

$$R = \left(\frac{\zeta\, E}{2\, n_0\, m_{H,He}\, (1+z_0)^3} \right)^{1/5} (\Delta t)^{2/5}\,.$$

$$\sim 10^{22.76} E_{57}^{1/5} z_{1.3}^{-3/5} (\Delta t)_{15}^{2/5}\,\mathrm{cm}$$

$$\zeta \;=\; 2.025\,, \quad m_{H,He} \;=\; 10^{-23.7}\mathrm{gm}$$

Hubble time at high redshift

$$t_H \;\sim\; 10^{16}\, z_{1.3}^{-3/2}\,\mathrm{s}\,.$$

Blast wave distance limit

$$R_{lim} \sim 10^{23.16} E_{57}^{1/5} z_{1.3}^{-6/5} \mathrm{cm}\,.$$

Energy density and particle content in the shell

$$\frac{E}{R^3} = \frac{B^2}{\eta_B 8\pi} = \frac{C}{\eta_{CR.e}} \frac{m_e c^2}{p-2}\,.$$

Spectral index of particle energy distribution, $p = 2.2$

$$B \approx 10^{-5.44} \eta_{B,-1}^{1/2} E_{57}^{1/5} z_{1.3}^{9/10} (\Delta t)_{15}^{-3/5}\ \mathrm{G}$$

$$C \approx 10^{-6.9} \eta_{CR,e,-1} E_{57}^{2/5} z_{1.3}^{9/5} (\Delta t)_{15}^{-6/5}\ \mathrm{cm}^{-3}$$

Radio luminosity per frequency

Parameter assumptions

The expressions for B and C assume that the energy transfer fractions for the electron and magnetic field instabilities are $\eta_{CR,e} = 0.1\eta_{CR,e,-1}$ and $\eta_B = 0.1\eta_{B,-1}$ respectively.

Pre-existing magnetic fields are assumed to be negligible

Expressions for luminosity per frequency

The radio luminosity, including the spectral k-correction $(1+z)^{1-0.6}$ (0.6 is the radio spectral index), is

$$L_\nu \;=\; 10^{30}\,\eta_{B,-1}^{0.8}\,\eta_{CR,e,-1}^{+1}\,E_{57}^{1.32}\,z_{1.3}^{1.84}\,\nu_{9.0}^{-0.6}\,(\Delta t)_{15}^{-0.96}\,\mathrm{erg\ s^{-1}\,Hz^{-1}}\,.$$

The factor $(\Delta t)_{15}$ can be written as $(\Delta t)_{15} \;\simeq\; 10\,z_{1.3}^{-3/2}$

$$L_\nu \;=\; 10^{29}\,\eta_{B,-1}^{0.8}\,\eta_{CR,e,-1}^{+1}\,E_{57}^{1.32}\,z_{1.3}^{3.34}\,\nu_{9.0}^{-0.6}\,\mathrm{erg\ s^{-1}\,Hz^{-1}}\,.$$

Luminosity per frequency after averaging over evolutionary stages

The emission is a function of time ($\sim t^{-1}$) so an average over the various evolutionary stages is required. Averaging introduces a factor of $\ln(t_{max}/t_{min})$

$$L_\nu \;=\; 10^{29.8}\,\eta_{B,-1}^{0.8}\,\eta_{CR,e,-1}^{+1}\,E_{57}^{1.32}\,z_{1.3}^{3.34}\,\nu_{9.0}^{-0.6}\,\mathrm{erg\ s^{-1}\,Hz^{-1}}\,.$$

Radio flux density

Expression for flux density in terms of luminosity

The radio background for a redshift interval of Δz is

$$F_\nu = N_{BH,0} \frac{c\, r(z)^2}{H(z)} \frac{L_\nu}{4\pi\, d_L^2} \Delta z \ \mathrm{erg\ s^{-1}\, Hz^{-1}\, cm^{-2}\, sr^{-1}}\,,$$

$$\begin{aligned} N_{BH,0} &= \mathrm{number\ \ density\ \ of\ \ explosions\ \ in\ \ co-moving\ \ frame} \\ L_\nu &= \mathrm{luminosity\ \ per\ \ frequency\ \ for\ \ a\ \ single\ \ explosion} \\ r(z) &= \mathrm{co-moving\ \ distance} \\ \Delta z &= \frac{2}{3}(1+z) = \mathrm{redshift\ \ interval\ \ over\ \ which\ \ the\ \ radio\ \ emission\ \ is\ \ maintained}\,. \end{aligned}$$

Flux density expression in terms of energy

At high redshift and for $N_{BH,0} = 1 N_{BH,0,0} \mathrm{Mpc}^{-3}$ and Hubble constant $h = 0.7$ the flux density can be written as

$$F_\nu \approx 10^{-19.8}\, N_{BH,0,0}\, \eta_{B,-1}^{0.8}\, \eta_{CR,e,-1}^{+1}\, E_{57}^{1.32}\, z_{1.3}^{0.84}\, \nu_{9.0}^{-0.6}\, \mathrm{erg\ s^{-1}\, Hz^{-1}\ cm^{-2}\, sr^{-1}}\,.$$

Condition required to match observed flux density at GHz level

Interpolating the observed flux density at the GHz level gives a flux density of

$$10^{-18.5}\,\mathrm{erg\ s^{-1}\,Hz^{-1}\ cm^{-2}\,sr^{-1}}\,.$$

Consistency between our model and observations requires that

$$10^{1.3} \;=\; N_{BH,0,0}\,\eta_{B,-1}^{0.8}\,\eta_{CR,e,-1}^{+1}\,E_{57}^{1.32}\,z_{1.3}^{0.84}$$

Uncertainties

The constant given above has large uncertainties:

- The value used for $N_{BH,0,0}$ may be too low.
- The value of z used ($z \sim 50$) may be too low. z may be as high as $z \sim 70$.
- The explosion energy could be higher or lower.
- The two efficiencies of creating magnetic fields or cosmic ray electrons from the explosion energy are conservative estimates.

Observational Checks

Upper limit on the strength of individual sources

Observational limit

The observational limit on the strength of individual sources is < 30 nJy .

Model prediction

The model predicts an energy density of

$$S_\nu = 10^{-31}\,\eta_{B,-1}^{0.8}\,\eta_{CR,e,-1}^{+1}\,E_{57}^{1.32}\,z_{1.3}^{-0.16}(\Delta t)_{15}^{-1}\,\nu_{9.0}^{-0.2}\mathrm{erg\ s^{-1}\,Hz^{-1}\ cm^{-2}}\,.$$

The average value is

$$S_\nu = 10^{-31.2}\,\eta_{B,-1}^{0.8}\,\eta_{CR,e,-1}^{+1}\,E_{57}^{1.32}\,z_{1.3}^{1.34}\,\nu_{9.0}^{-0.2}\mathrm{erg\ s^{-1}\,Hz^{-1}\ cm^{-2}}\,.$$

This corresponds to a flux density of < 20 nJy .
The corresponding far infrared emission must be negligible.

Number of sources

Number of sources per solid angle

The number of sources per solid angle is

$$N_{obs} = 10^{9.8}\, N_{Bh,0,0}\, z_{1.3}^{-1/2}\,, \quad \Delta z/(1+z) = 2/3\,.$$

Discrepancy between theory and observations

The predicted value is below the observed value of $10^{11.8}\,\mathrm{sr}^{-1}$.

The sources in our model are not point sources. They overlap substantially, so they are missed by searches for compact sources.

Beam smearing

The angular size of the remnants in our model is

$$\theta = 10^{-4.2}\, E_{57}^{1/5}\, z_{1.3}^{-1/5}\,\mathrm{rad} \approx 12\,\mathrm{arcsec}\,.$$

The observed value for the number of sources was obtained by using a beam of 8 arcsec resolution.

The requirement that the diameter of the sources be less than a resolution element is equivalent to the restriction of the time element to an interval which is 10^{-5} times the full time of evolution.

The flux density is higher by $10^{4.2}$, but it is within the observed limits.

Number of sources in the relativistic growth phase of early expansion

The number of sources in the relativistic growth phase can be estimated by choosing the time interval for this phase to be that at which the blast-wave becomes non-relativistic

$$(\Delta t)_{15} \sim 10^{-5} E^{1/3} z_{1.3}^{-1} .$$

At high redshift the time-redshift relation can be expanded as

$$\Delta t = \tau_H \frac{3}{2}(1+z)^{-5/2} \Delta z .$$

When these two expressions for Δt are equal,

$$\Delta z \simeq 10^{-4.6} E_{57}^{1/3} z_{1.3}^{3/2} .$$

From this expression for Δz the number of sources in the relativistic phase is found to be $10^{3.3} N_{BH,0,0}$ independent of redshift.

Number of sources per angular resolution element

The number of sources per angular resolution element is of the order of $10^{3.3}\, N_{BH,0,0}\, z_{1.3}^{-1/2}$

This implies that considerable smearing will occur.

By Poisson noise alone the fractional residual flux variations will be $\simeq 10^{-1}$.

Correspondingly, the equivalent source number density increases by 10^2, raising the previous estimate from $10^{9.8}\mathrm{sr}^{-1}$ to $10^{11.8}\mathrm{sr}^{-1}$.

The very early, brief phases of the evolution are the only ones during which the flux density comes close to the current survey limits.

Reproduction of observed spectrum

Energy gain and loss by scattering

The observed radio spectrum implies a particle spectrum of $E^{-2.2}$.

In our model the power of E is -2.24, which arises from summing the contributions to a relativistic particle's energy from a strong, plane-parallel shock in a gas and from the drift energy gain .

The corresponding radio frequency dependence of the spectrum in our model is $\nu^{-0.62}$, and the observed radio frequency dependence is $\nu^{-0.599}$.

Additional Features of the Model

The observed mass distribution of super-massive black holes can be explained analytically as a merger sequence.

When super-massive black holes merge, their spins are uncorrelated, and therefore the spin of the resulting black hole is dominated by the orbital spin of the merging black holes.

The dominant spin precesses and sweeps out a cone, producing ultra-high energy cosmic rays whose interactions are a source of high energy γ-rays and neutrinos.

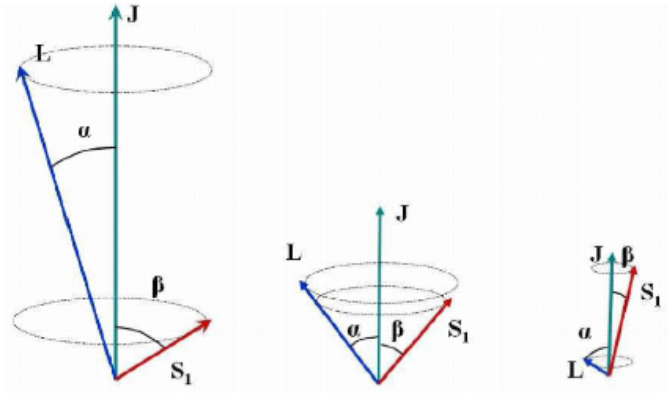

FIG. 1: The spin-flip phenomenon in black hole binary mergers: Individual BH spin is $\boldsymbol{S}$, orbital angular momentum is $\boldsymbol{L}$, and total angular momentum is $\boldsymbol{J}$. These three steps show the envisaged **temporal evolution of the final stages of the merger, as the jet direction $\boldsymbol{S}$ sweeps around**. Source: L.A. Gergely & P.Biermann 2009 ApJ

The sweeping action has been observed in M82 around the compact source 41.9+58. This event may be the source of the UHECR protons detected by the Telescope Array. This is a merger of the type which produced the gravitational wave event most recently reported on by LIGO, two merging stellar-mass black holes with uncorrelated spin. This is most likely to happen in a dense star cluster if young, massive stars. Massive stars are observed to be in binary systems with short periods. When two or more binary systems interact, stars and black holes can be exchanged between systems.

When radio jets are pointed towards earth, the radio spectrum is flat. A small sample of the merging super-massive black hole binaries exhibits such a flat spectrum to near the THz range.

A correlation of the flat spectrum radio sources with track event neutrinos (those with good pointing) yields four sources, two of which have a flat spectrum to near the THz range, consistent with our model.

Conclusions

Non-thermal radio background from high redshift super-massive black holes

The formation of the first generation of super-massive black holes in our model is assumed to produce radio remnants which are scaled-up versions of normal supernova remnants .

Our model satisfies all known observational constraints; .

Single-source strength.

Total number.

Lack of far-infrared emission.

Other backgrounds

Our model also explains the neutrino background and possibly explains the observed flux density and spectrum of the $\gamma-$ray background.

Strong constraints on the efficiency factor $\eta_B^{0.8}\,\eta_{CR,e}/\eta_{CR}$ are obtained by matching both the neutrino spectrum and the radio background spectrum .

The merger of two super-massive black holes results in the production of gravitational waves, UHECRs and neutrinos. In addition to the observed broad energy range for the massive particles and the associated radio background there should be a gravitational wave background with a broad range of frequencies.